

CONFIDENTIAL

4  
Copy  
RM L58B04

UNCLASSIFIED.

c2



# RESEARCH MEMORANDUM

FREE-FLIGHT INVESTIGATION TO DETERMINE THE INLET  
EXTERNAL DRAG OF FOUR INLET MODELS AT  
MACH NUMBERS FROM 1.50 TO 3.00

By Walter L. Kouyoumjian

Langley Aeronautical Laboratory  
Langley Field, Va.

**LIBRARY COPY**

APR 21 1958

LANGLEY AERONAUTICAL LABORATORY  
LIBRARY, NACA  
LANGLEY FIELD, VIRGINIA

CLASSIFIED DOCUMENT

This material contains information affecting the National Defense of the United States within the meaning of the espionage laws, Title 18, U.S.C., Secs. 793 and 794, the transmission or revelation of which in any manner to an unauthorized person is prohibited by law.

**NATIONAL ADVISORY COMMITTEE  
FOR AERONAUTICS**

WASHINGTON

April 21, 1958

CONFIDENTIAL

CLASSIFICATION CHANGED  
UNCLASSIFIED

By authority of JAGG 4-5-58 Date

UNCLASSIFIED

NACA RM L58B04

NACA RM L58B04

## NATIONAL ADVISORY COMMITTEE FOR AERONAUTICS

## RESEARCH MEMORANDUM

## FREE-FLIGHT INVESTIGATION TO DETERMINE THE INLET

## EXTERNAL DRAG OF FOUR INLET MODELS AT

## MACH NUMBERS FROM 1.50 TO 3.00

By Walter L. Kouyoumjian

## SUMMARY

A free-flight investigation was conducted of four supersonic nose inlets. Each inlet used conical-shock and isentropic-compression center bodies in various combinations. Two of the models investigated had internal contraction and two did not; three were designed for a free-stream Mach number of 3.00 while one was designed for a free-stream Mach number of 2.60.

The models were flight tested at zero angle of attack at Mach numbers varying between 1.50 and 3.00. The Reynolds number range for the flight tests was from  $5 \times 10^6$  to  $15 \times 10^6$ , based on body maximum diameter. The performance characteristics of the inlets are presented as the variation of drag coefficient, total-pressure recovery, and mass-flow ratio over the Mach number range. Only one inlet model (conical shock plus isentropic compression with internal contraction) achieved a mass-flow ratio of 1.00 at the design Mach number of 3.00.

## INTRODUCTION

As part of a general program of the National Advisory Committee for Aeronautics to determine the aerodynamic characteristics of high-speed inlets, the Pilotless Aircraft Research Division has flight tested models of several inlet configurations at supersonic speeds. Reference 1 presents the effects of cowl profile shape and inlet mass-flow ratio on the drag of normal-shock nose inlets for Mach numbers from 0.9 to 1.5. Reference 2 presents the results of the investigation of conical-shock external-compression inlets at flight Mach numbers between 0.8 and 2.0.

The present investigation was conducted to determine the inlet external drag of four models at Mach numbers between 1.50 and 3.00. Three of the inlets investigated, a conical inlet with internal compression, a combination conical-isentropic inlet with internal compression, and a combination conical-isentropic inlet without internal compression, were designed for a Mach number of 3.00. The fourth inlet, which also was a combination conical-isentropic inlet without internal compression, was designed for a Mach number of 2.60. This paper presents the inlet external-drag, pressure-recovery, and mass-flow ratio data for the individual fixed-geometry inlets.

## SYMBOLS

A	area, sq ft
$a_l$	longitudinal acceleration, g units
$C_{D,t}$	total-drag coefficient, $\frac{\text{Total drag}}{q_\infty S}$
$C_{D,b}$	base-drag coefficient, $\frac{\text{Base drag}}{q_\infty S}$
$C_{D,i}$	internal-drag coefficient, $\frac{\text{Internal drag}}{q_\infty S}$
$C_{D,f}$	skin-friction drag coefficient, $\frac{\text{Skin-friction drag}}{q_\infty S}$
$C_{D,W}$	fin-drag coefficient, $\frac{\text{Fin drag}}{q_\infty S}$
$C_{D,x}$	inlet external-drag coefficient, $C_{D,t} - C_{D,b} - C_{D,i} - C_{D,f} - C_{D,W}$
M	Mach number
p	static pressure, lb/sq ft
$p_t$	total pressure, lb/sq ft

q	dynamic pressure, $\frac{1}{2}\rho V^2$ , lb/sq ft
R	Reynolds number based on maximum body diameter
S	maximum projected area, 0.267 sq ft
W	weight of model, lb
$\frac{W}{W_\infty}$	mass-flow ratio (ratio of actual inlet mass flow to maximum theoretical mass flow based on inlet capture area)
X	station measured from leading edge of cowl, in.
$X_R$	station measured from leading point of center body, in.
$Y_R$	radius coordinate for center body and cowl, measured from longitudinal axis, in.

## Subscripts:

$\infty$	free stream
d	subsonic diffuser exit; entrance to convergent-divergent exit nozzle
e	nozzle exit station
o	inlet entrance station
N	nozzle throat station
b	base annulus

## MODELS AND APPARATUS

General sketches of the four inlets investigated appear in figure 1 and photographs of the models are presented in figure 2. A typical model-launcher arrangement is shown in figure 3.

The four inlet models were designed to be similar in order to facilitate the analysis of the results of the investigation. Each model was stabilized in flight by four 60° sweptback fins with a taper ratio of 0.1175; the fins were made of aluminum and had tapered leading and

trailing edges. The rearward section of the fuselage for each model was a straight cylindrical section constructed of spun steel sheet of constant thickness, and had a maximum external diameter of 7.00 inches; the cowl profiles for the separate inlets (also of spun steel sheet) were faired into the fuselage at different axial locations. (See fig. 1.) Figure 4 presents the internal area distribution for the inlet models investigated.

The subsonic diffuser sections for all the models were designed to give uniform flow at the diffuser exit. The nozzle was designed to give choking flow at a free-stream Mach number of 1.50 or greater, and under these conditions gave an exit Mach number of 2.02.

Model A had a single-cone center body with a cone half-angle of  $25^\circ$  and internal contraction ratio of 1.15. The inlet design Mach number was 3.00 and was defined as the Mach number at which the initial conical shock from the center-body point would intersect with the cowl leading edge. The cowl for this inlet had a sharp leading edge and was faired into the straight cylindrical section of the fuselage at a distance of 10.13 inches behind the cowl leading edge. The coordinates for the center body are presented in table I and the internal cowl dimensions in figure 1(a). The cowl profile for model A was a straight conic section; therefore, the cowl coordinates were omitted from table I.

Model B had a center body with an initial cone half-angle of approximately  $15^\circ$  followed by sufficient isentropic compression to reduce the Mach number on the external compression surface to a theoretical value of 1.76 at the entrance of the inlet at the design Mach number of 3.00. This inlet was designed from the results of reference 3. The center body was similar to center body III and the cowl was similar to cowl III<sub>a</sub> in reference 3. The external cowl surface made an angle of  $35^\circ$  with the inlet center line at the leading edge of the cowl. The coordinates for the center body and the interior of the cowl are presented in table II.

Model C had an isentropic center body with an initial cone half-angle of approximately  $15^\circ$  followed by enough isentropic compression to reduce the surface Mach number to 1.50 at the entrance to the inlet for a design Mach number of 3.00. This inlet was similar to center body IV<sub>a</sub> and cowl IV of reference 3 and did not have any internal compression. The external angle between the cowl surface and the inlet center line was  $30^\circ$  at the cowl leading edge. The coordinates for cowl and center body are presented in table III.

Model D had an isentropic center body with an initial cone half-angle of  $6.7^\circ$  followed by  $29.3^\circ$  of isentropic compression. The inlet did not have any internal compression, and the design Mach number was 2.60. The coordinates for the center body are given in table IV. The

cowl profile for this inlet was a circular arc of 11.523-inch radius that was faired into the cylindrical section of the fuselage.

#### DATA REDUCTION

The values of total-drag coefficient for the models were computed during decelerating flight from the telemetered longitudinal accelerometer data and the equation

$$C_{D,t} = \frac{W a_l}{q_\infty S} \quad (1)$$

For comparative purposes the total-drag-coefficient values were also determined from acceleration data obtained by differentiating the CW Doppler radar velocity measurements (corrected for flight-path curvature and winds aloft) and the NACA modified SCR-584 radar trajectory measurements. The details of the testing technique are presented in reference 4. Since the CW Doppler failed to track the models throughout the test range, this method for computing the total-drag coefficient was useful only in verifying the coefficients obtained from the accelerometer data at the high supersonic speeds. The agreement between total-drag coefficients computed by both methods was within instrument accuracy, and the total-drag coefficients presented in this report were computed from the accelerometer data.

The inlet mass-flow ratios were computed from the telemetered average total-pressure data taken at the entrance of the convergent-divergent nozzle during the flight. The equation used was

$$\frac{W}{W_\infty} = \frac{(0.5283)(1.095)p_{t,d} A_N}{p_\infty M_\infty (1 + 0.2 M_\infty^2)^{1/2} A_O} \quad (2)$$

Equation (2) assumed choking flow at the nozzle throat and no total-pressure loss through the convergent-divergent exit nozzle.

The internal-drag coefficient was computed from the one-dimensional form of the momentum equation, applied between free-stream conditions and conditions at the exit of the model:

$$C_{D,i} = 2 \left[ \frac{w}{w_\infty} \frac{A_o}{S} - \frac{(0.1239)p_{t,e}(2.02)^2 A_e}{p_\infty M_\infty^2 S} - \frac{1}{1.4 M_\infty^2} \frac{A_e}{S} \left( \frac{0.1239 p_{t,e}}{p_\infty} - 1 \right) \right] \quad (3)$$

where 2.02 is the exit Mach number.

The base drag coefficient for the models was computed by using the following equation:

$$C_{D,b} = - \frac{(p_b - p_\infty) A_b}{q_\infty S} \quad (4)$$

The inlet total-pressure recovery was taken as the ratio of the total pressure measured at the diffuser exit station to the total pressure of the stream-tube air upstream of the inlet.

The skin-friction drag coefficient was computed by the method outlined in reference 5. It was assumed that the boundary layer was fully turbulent over the entire model. The fin-drag coefficient was estimated from data presented in reference 6.

The inlet external-drag coefficient was taken as the difference between the total-drag coefficient and the component-drag coefficients for each model, or

$$C_{D,x} = C_{D,t} - C_{D,i} - C_{D,b} - C_{D,f} - C_{D,w} \quad (5)$$

This results in an external-drag-coefficient term that is composed of the dragwise components of (1) the aerodynamic pressure and viscous forces acting on the external surfaces of the inlet and (2) the aerodynamic forces acting on the external contours of the stream tube entering the inlet between the shock wave and the cowl lip (additive-drag component).

The data presented herein are believed to be accurate within the following limits:

$\frac{w}{w_\infty}$ . . . . .	±0.02
$C_D$ . . . . .	±0.01
$M_\infty$ . . . . .	±0.01

## RESULTS

The components of drag coefficient for the four inlets investigated are plotted against free-stream Mach number in figures 5 to 8. The mass-flow ratio, total-pressure recovery, and Reynolds number range for these inlets are also presented in figures 5 to 8. All the models except model A attained their design Mach numbers in flight.

The curves of the mass-flow ratio for each of the inlets investigated show that only inlet B operated at a maximum mass-flow ratio of 1.00 at its design Mach number. An extrapolation of the mass-flow-ratio curve for model A (fig. 5) indicates that the mass-flow ratio would be approximately equal to 1.00 at the inlet design Mach number. Inlet C operated at a mass-flow ratio of 0.84 at a free-stream Mach number of 3.00 and inlet D operated at a mass-flow ratio of 0.88 at a free-stream Mach number of 2.60. The limited nature of the present investigation does not allow rigorous analysis of the inlet performance characteristics.

As defined previously, the inlet external-drag coefficient contains the dragwise component of the pressure and viscous forces on the inlet plus the aerodynamic pressure forces on the streamline of the stream tube entering the inlet, the latter component being with "additive-drag" term. An estimate of the additive-drag component of the inlet external drag was made for the conical inlet, model A, by using the results presented in reference 7, and the curve is presented in figure 5. The additive-drag coefficients were not estimated for models B, C, and D, since the isentropic-compression surfaces of their center bodies greatly complicated the computation of the additive-drag coefficients. The inclusion of additive drag in the inlet external-drag coefficient gives values which may be of practical importance to an aircraft designer who desires information on the off-design performance penalties of a particular type of fixed-geometry inlet. Figure 9 is a convenient summary of the inlet external-drag coefficients for the four inlets investigated.

## CONCLUDING REMARKS

The inlet external-drag coefficients and the component-drag coefficients are presented for the inlets investigated over a flight Mach number range of 1.50 to 3.00. The inlet external-drag coefficient contains the "additive-drag" component. The models were fixed-geometry annular inlets; three of them were designed for a free-stream Mach number of 3.00 and one was designed for a free-stream Mach number of 2.60.



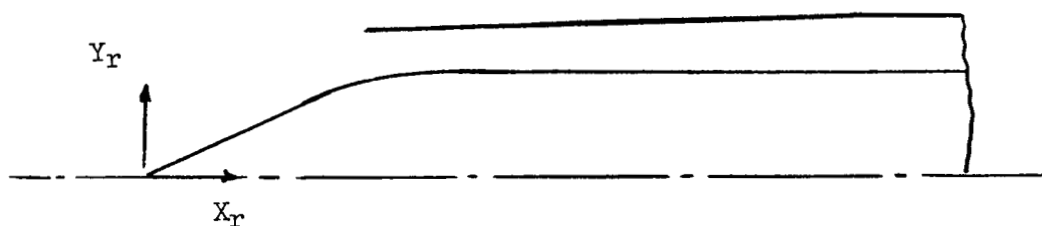
The curves of the mass-flow ratio for the four inlets indicated that only model B operated at maximum mass-flow ratio at its inlet design Mach number (3.00), although the trend of the curve for inlet A indicated that it might also operate at a mass-flow ratio of 1.00 at its inlet design Mach number of 3.00, and neither model C nor model D operated at maximum mass-flow ratio at or near the design Mach number.

Langley Aeronautical Laboratory,  
National Advisory Committee for Aeronautics,  
Langley Field, Va., January 14, 1958.

#### REFERENCES

1. Sears, R. I., Merlet, C. F., and Putland, L. W.: Flight Determination of Drag of Normal-Shock Nose Inlets With Various Cowling Profiles at Mach Numbers From 0.9 to 1.5. NACA Rep. 1281, 1956. (Supersedes NACA RM L53I25a.)
2. Merlet, Charles F., and Putland, Leonard W.: Flight Determination of the Drag of Conical-Shock Nose Inlets With Various Cowling Shapes and Axial Positions of the Center Body at Mach Numbers From 0.8 to 2.00. NACA RM L54G21a, 1954.
3. Hunczak, Henry R.: Pressure Recovery and Mass-Flow Performance of Four Annular Nose Inlets Operating in Mach Number Region of 3.1 and Reynolds Number Range of Approximately  $0.45 \times 10^6$  to  $2.20 \times 10^6$ . NACA RM E54A07, 1954.
4. Wallskog, Harvey A., and Hart, Roger G.: Investigation of the Drag of Blunt-Nosed Bodies of Revolution in Free Flight at Mach Numbers From 0.6 to 2.3. NACA RM L53D14a, 1953.
5. Van Driest, E. R.: Turbulent Boundary Layer in Compressible Fluids. Jour. Aero. Sci., vol. 18, no. 3, Mar. 1951, pp. 145-160, 216.
6. Hopko, Russell N., and Sandahl, Carl A.: Free-Flight Investigation of the Zero-Lift Drag of Several Wings at Supersonic Mach Numbers Extending to 2.6. NACA RM L52D29, 1952.
7. Sibulkin, Merwin: Theoretical and Experimental Investigation of Additive Drag. NACA Rep. 1187, 1954. (Supersedes NACA RM E51B13.)

TABLE I.- COORDINATES FOR MODEL A



Center-body coordinates

$X_r$	$Y_r$
0	0
Straight taper	
4.225	1.968
4.325	2.016
4.425	2.061
4.525	2.112
4.625	2.153
4.725	2.192
4.825	2.229
4.925	2.263
5.025	2.291
5.125	2.318
5.225	2.339
5.325	2.359
5.425	2.371
5.525	2.383
5.625	2.391
5.725	2.396
5.825	2.398
5.925	2.399
6.025	2.400
Straight taper	
20.622	2.366

TABLE II.- COORDINATES FOR MODEL B

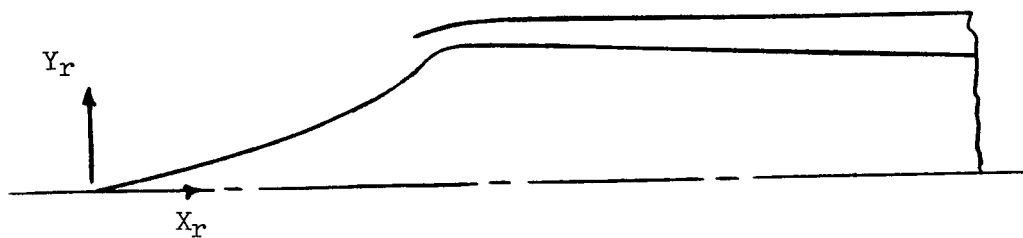
Cowl coordinates  
(internal)

$X_r$	$Y_r$
6.222	2.875
6.546	3.015
6.795	3.113
7.178	3.233
7.562	3.325
7.945	3.394
8.328	3.435
8.712	3.450

Center-body coordinates

$X_r$	$Y_r$
0	0
Straight taper	
2.875	.776
3.450	.947
4.025	1.135
4.600	1.357
5.175	1.633
5.500	1.834
5.702	1.957
Straight taper	
6.352	2.415
6.517	2.517
6.900	2.720
7.283	2.869
7.667	2.978
8.245	3.079
8.817	3.087
Straight taper	
22.000	2.366

TABLE III.- COORDINATES FOR MODEL C

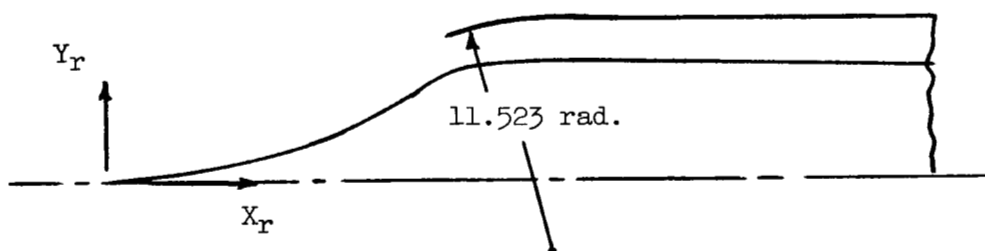
Cowl coordinates  
(internal)

$X_r$	$Y_r$
6.751	3.165
Straight taper	
6.808	3.201
6.904	3.251
7.000	3.289
7.096	3.320
7.192	3.347
7.288	3.366
7.384	3.383
7.479	3.396
7.671	3.419
7.863	3.433
8.054	3.442
8.246	3.446
8.668	3.450

Center-body coordinates

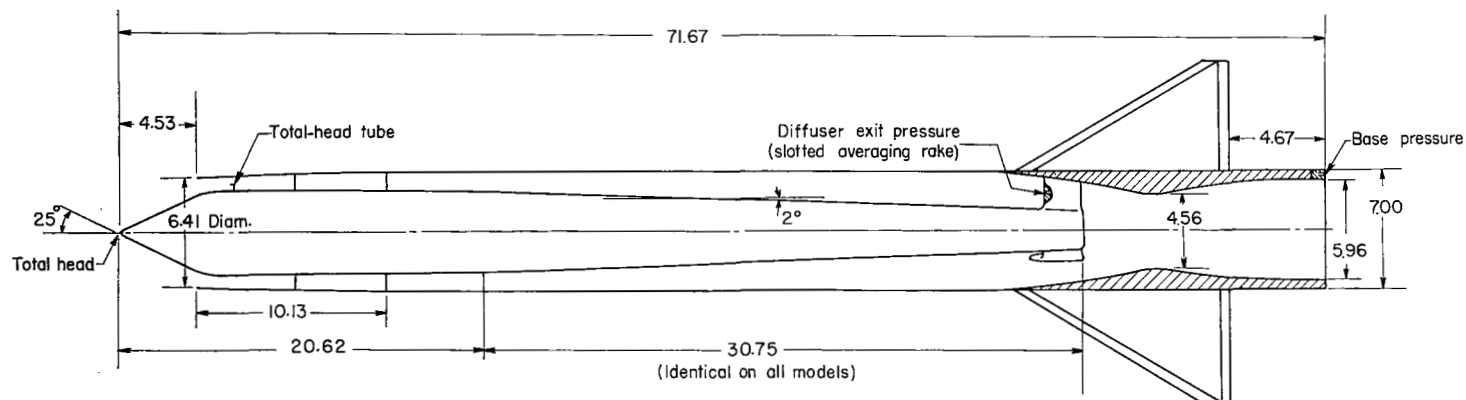
$X_r$	$Y_r$
0	0
.479	.125
.958	.255
1.438	.381
1.917	.510
2.396	.638
2.875	.767
3.354	.899
3.833	1.041
4.313	1.196
4.792	1.369
5.271	1.568
5.750	1.806
6.133	2.036
6.325	2.170
6.517	2.321
6.708	2.492
6.900	2.668
6.996	2.750
7.092	2.816
7.188	2.864
7.283	2.896
7.475	2.929
7.667	2.946
8.050	2.963
8.625	2.971
9.583	2.952
10.542	2.923
Straight taper	
22.528	2.366

TABLE IV.- COORDINATES FOR MODEL D

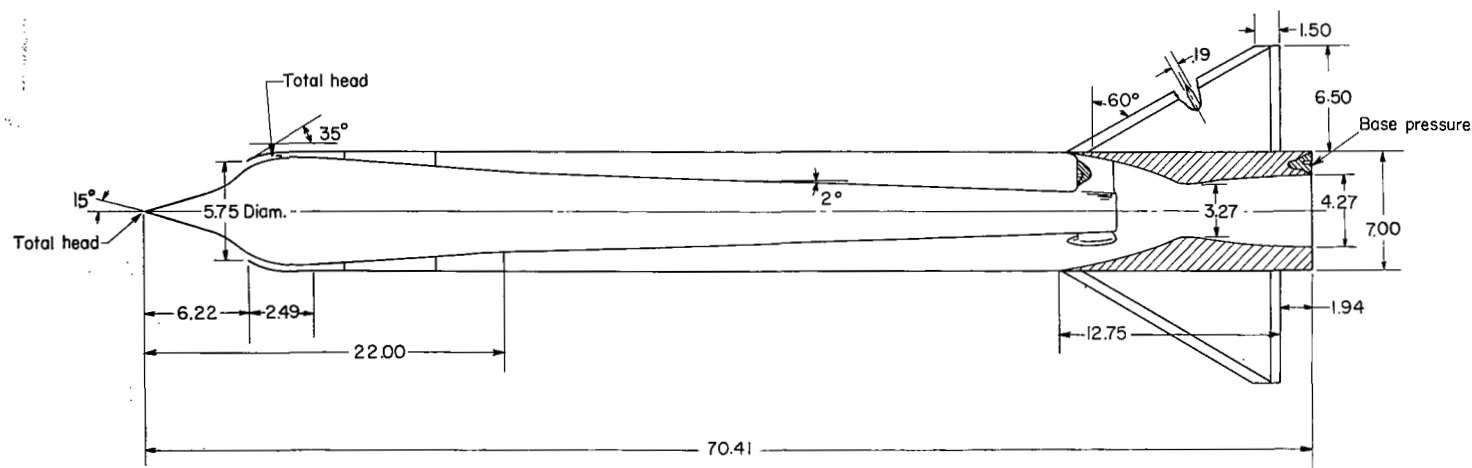


Center-body coordinates

$X_r$	$Y_r$
0	0
.493	.058
.986	.123
1.480	.202
1.971	.294
2.466	.394
2.959	.511
3.485	.639
3.946	.779
4.439	.943
4.932	1.130
5.426	1.344
5.918	1.595
6.412	1.891
6.659	2.060
7.255	2.339
8.985	2.568
9.266	2.561
Straight taper	
22.526	2.366

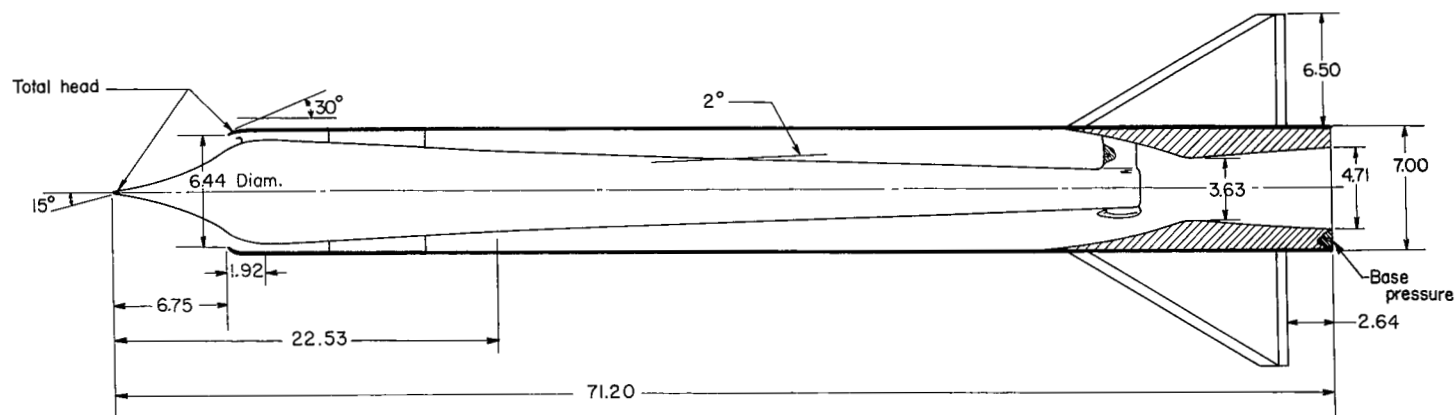


Model A

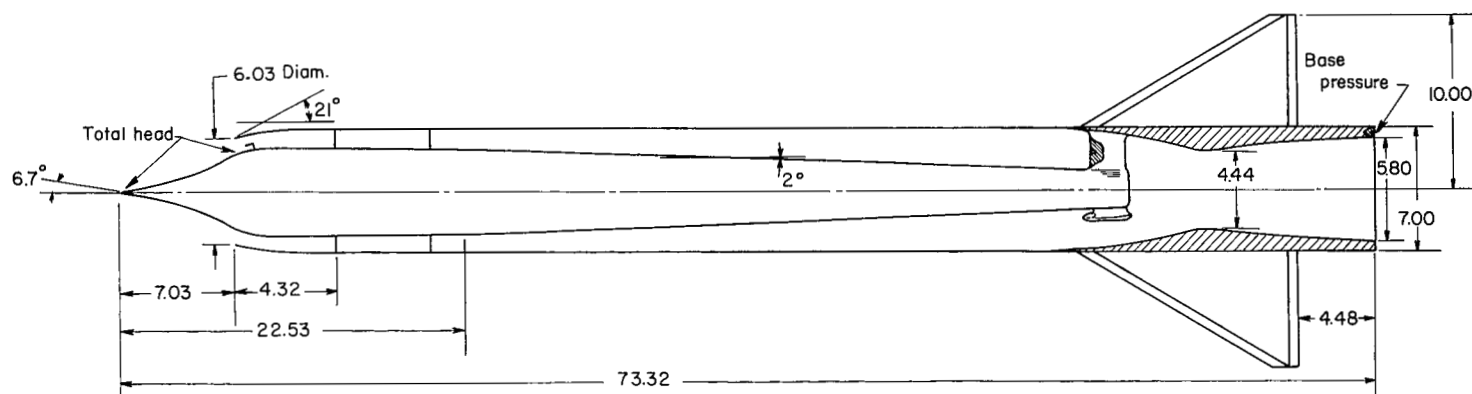


Model B

Figure 1.- General sketch of models. All dimensions are in inches.

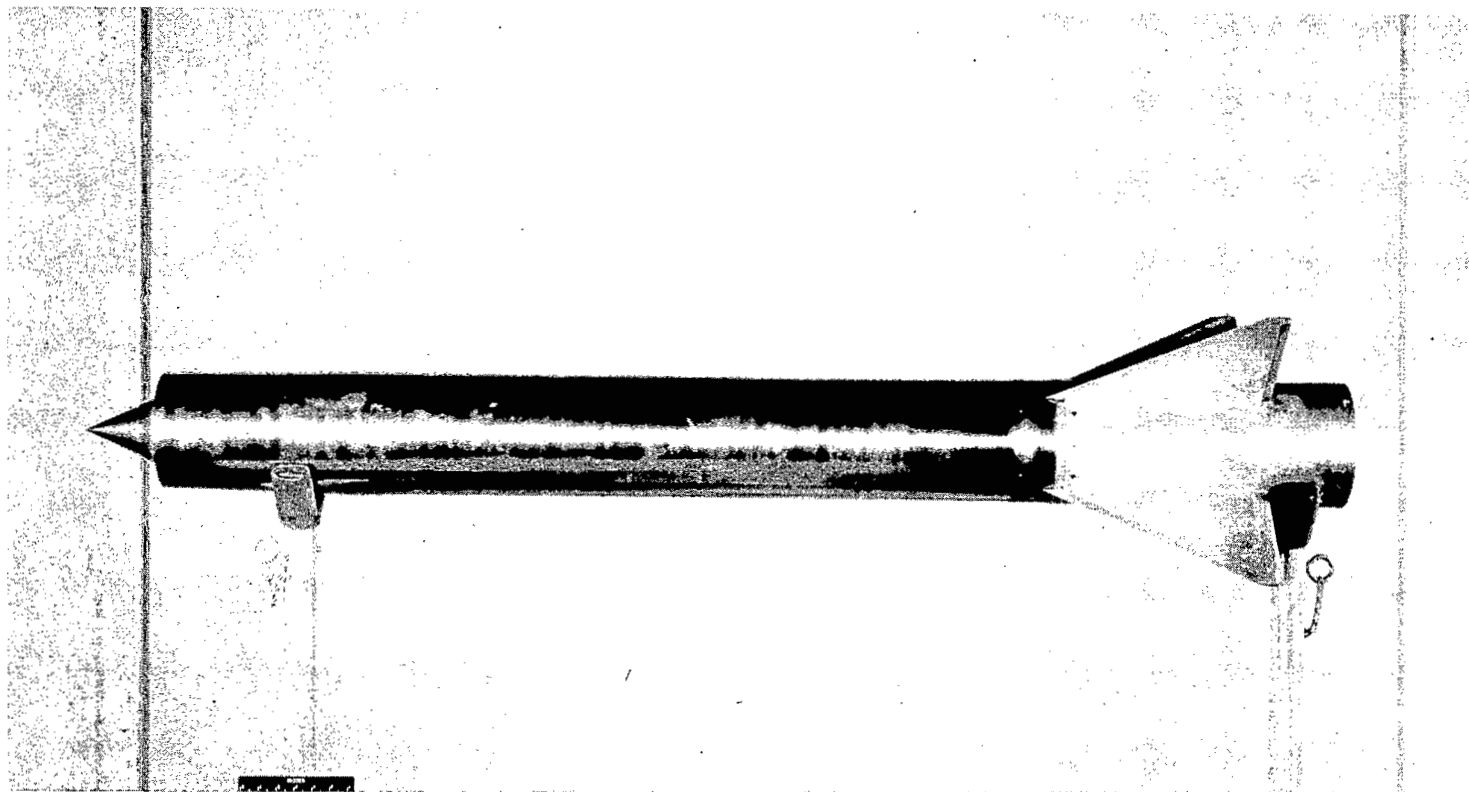


Model C



Model D

Figure 1.- Concluded.



Side view

L-92151.1

(a) Model A.

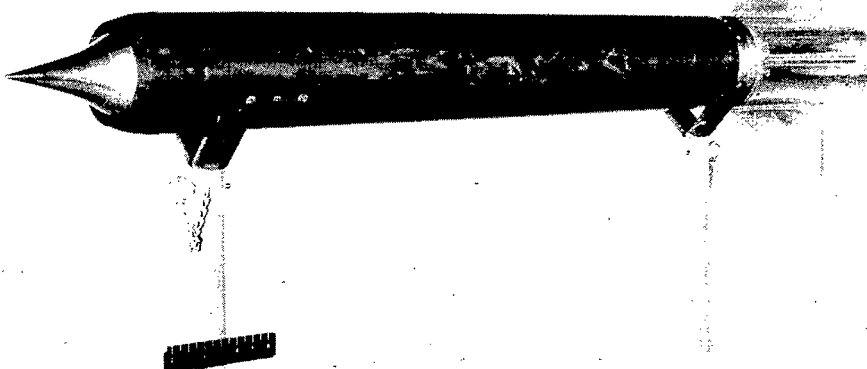
Figure 2.- Photographs of models.





Side view

L-95060

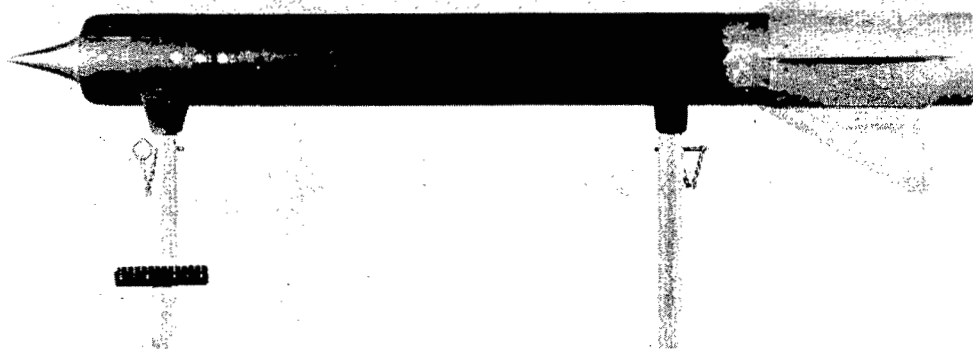


Oblique view

L-95061

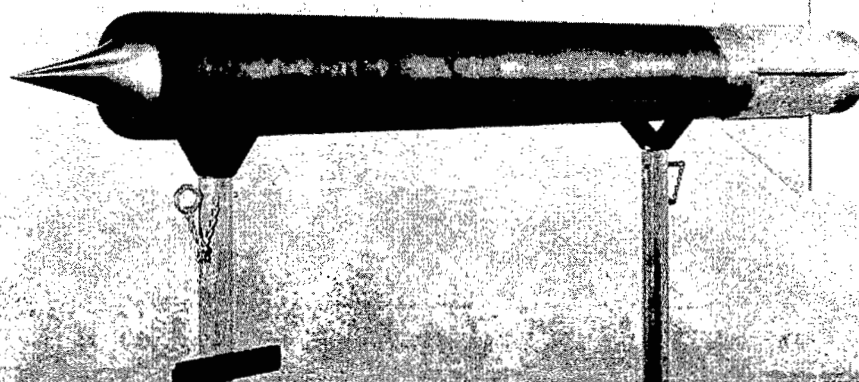
(b) Model B.

Figure 2.- Continued.



Side view

L-94782

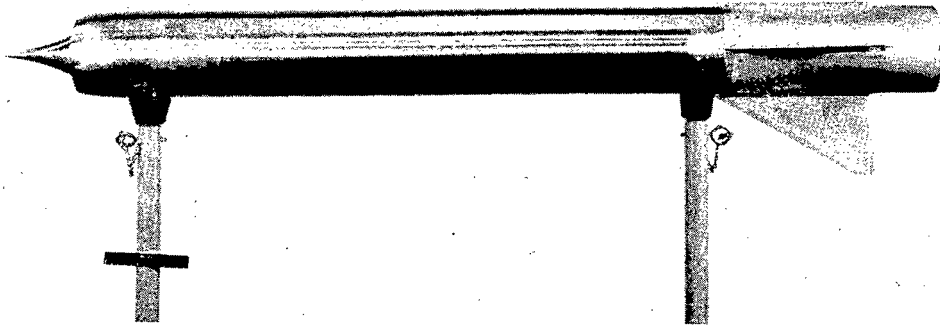


Oblique view

L-94784

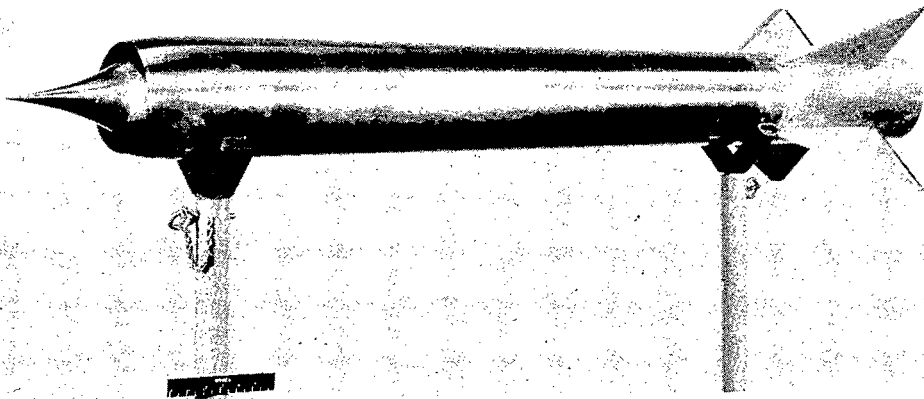
(c) Model C.

Figure 2.- Continued.



Side view

L-94388



Oblique view

L-94389

(d) Model D.

Figure 2.- Concluded.

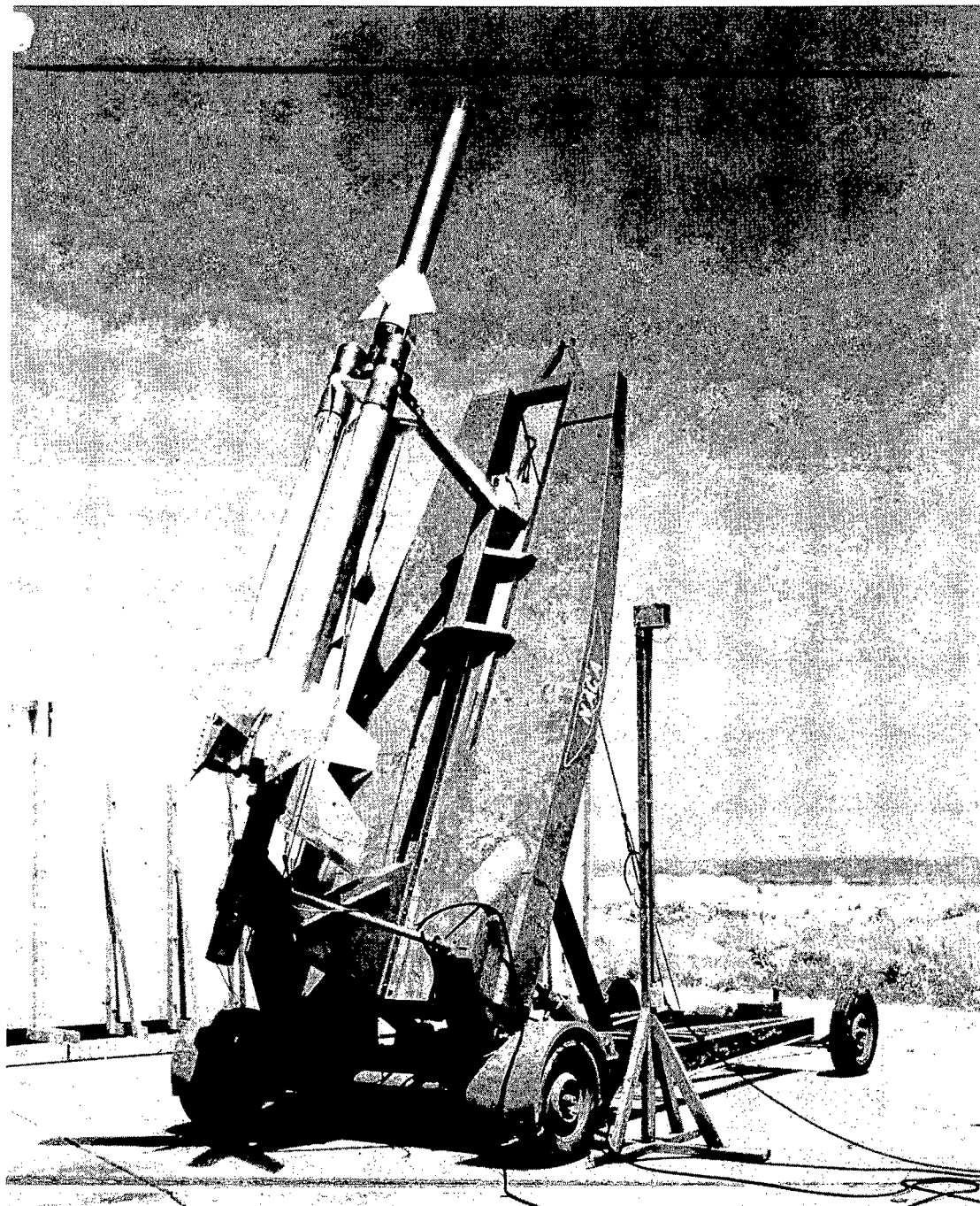


Figure 3.- Typical model on launcher.

L-94546.1

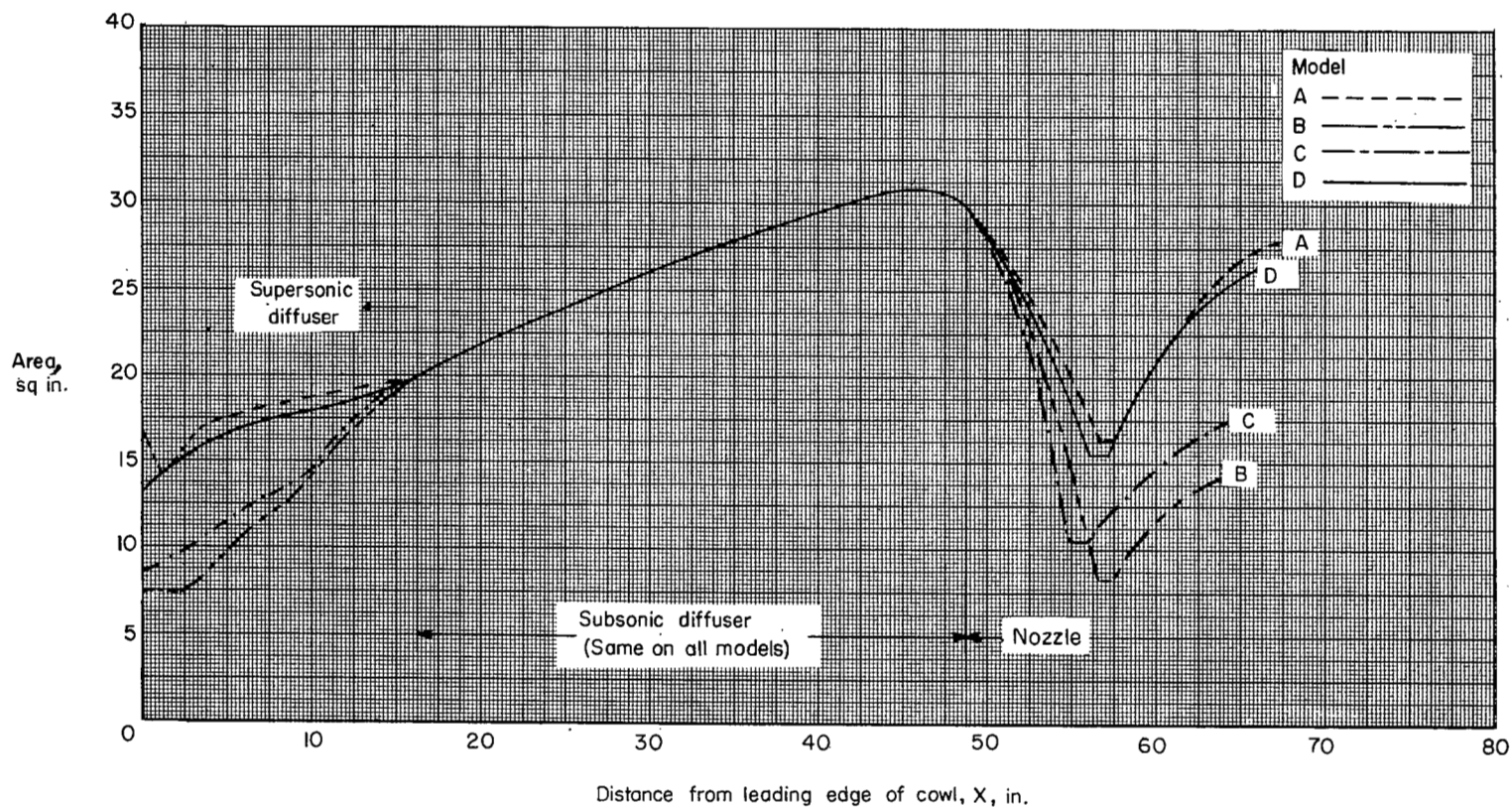


Figure 4.- Area distribution.

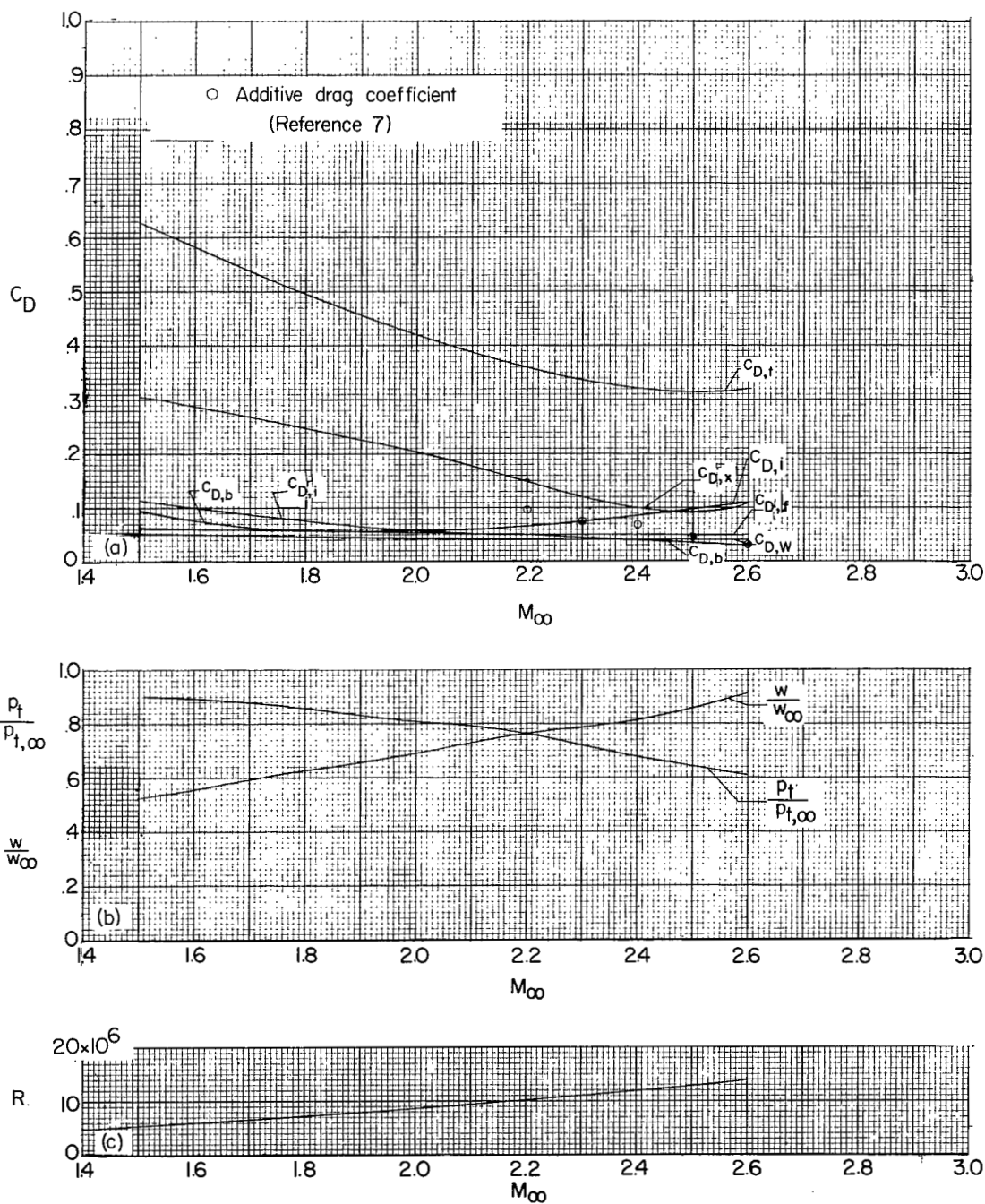


Figure 5.- Variation of drag-coefficient components, mass-flow ratio, pressure recovery, and Reynolds number with free-stream Mach number. Model A.

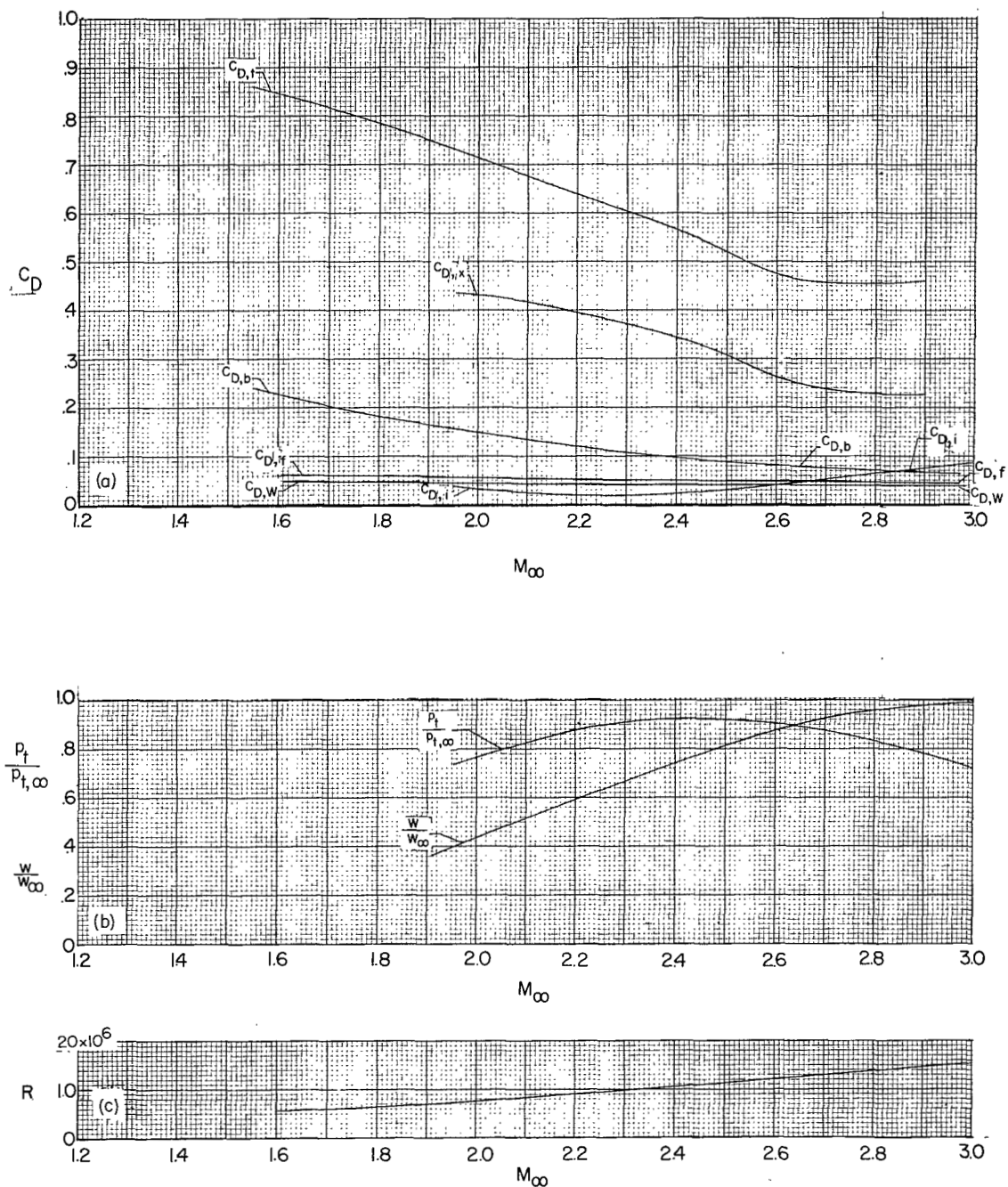


Figure 6.- Variation of drag-coefficient components, mass-flow ratio, pressure recovery, and Reynolds number with free-stream Mach number. Model B.



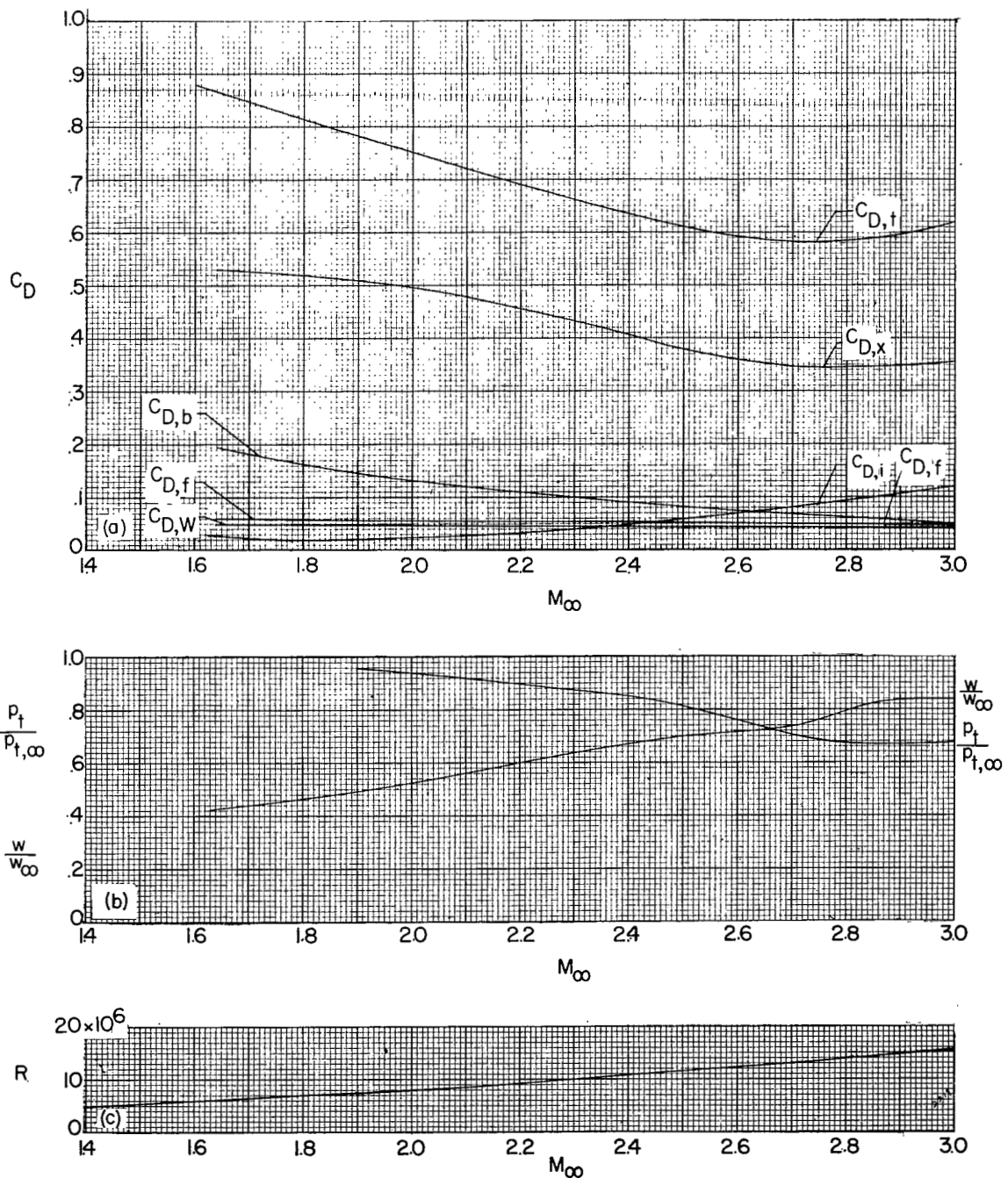


Figure 7.- Variation of drag-coefficient components, mass-flow ratio, pressure recovery, and Reynolds number with free-stream Mach number. Model C.



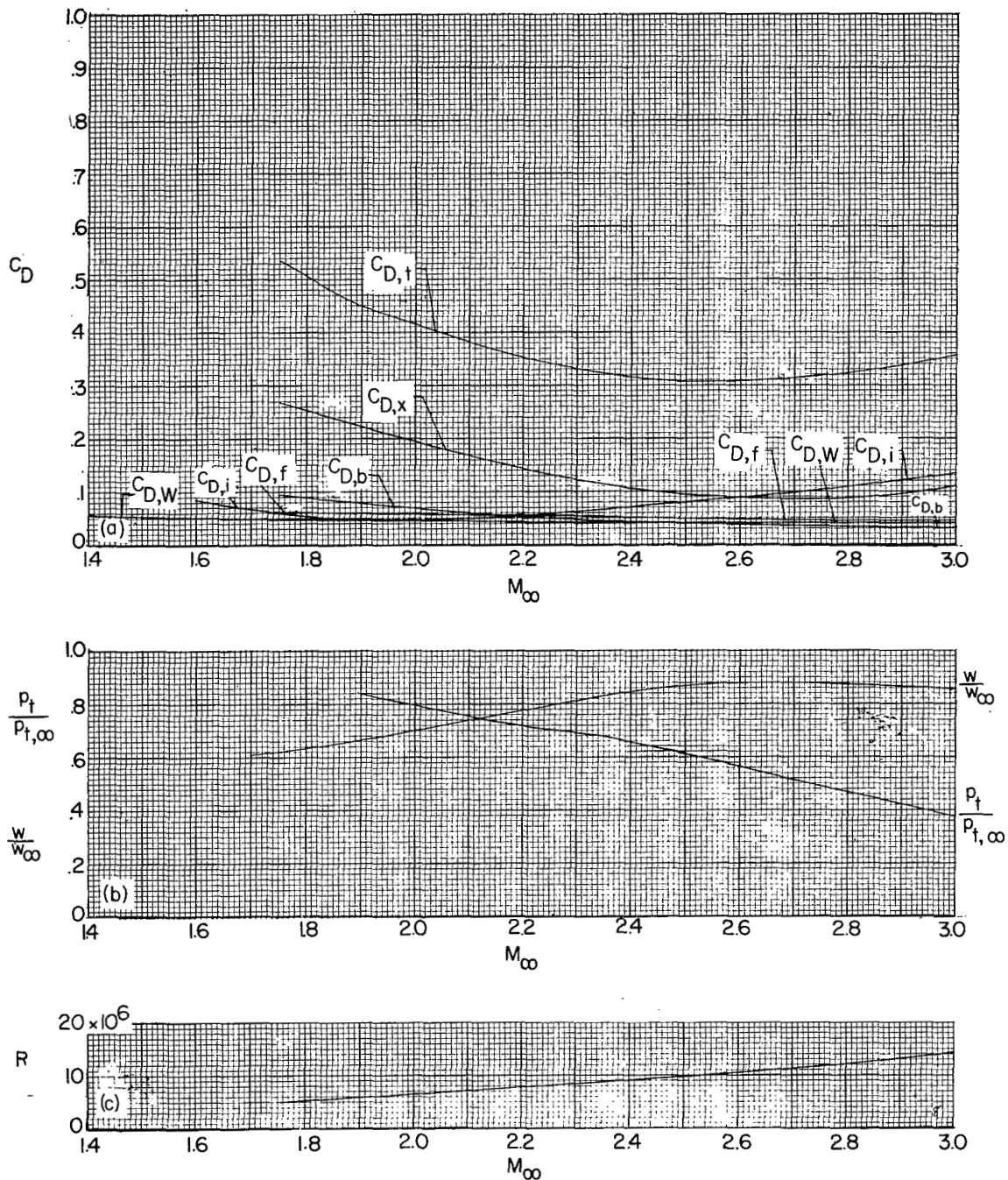


Figure 8.- Variation of drag-coefficient components, mass-flow ratio, pressure recovery, and Reynolds number with free-stream Mach number. Model D.

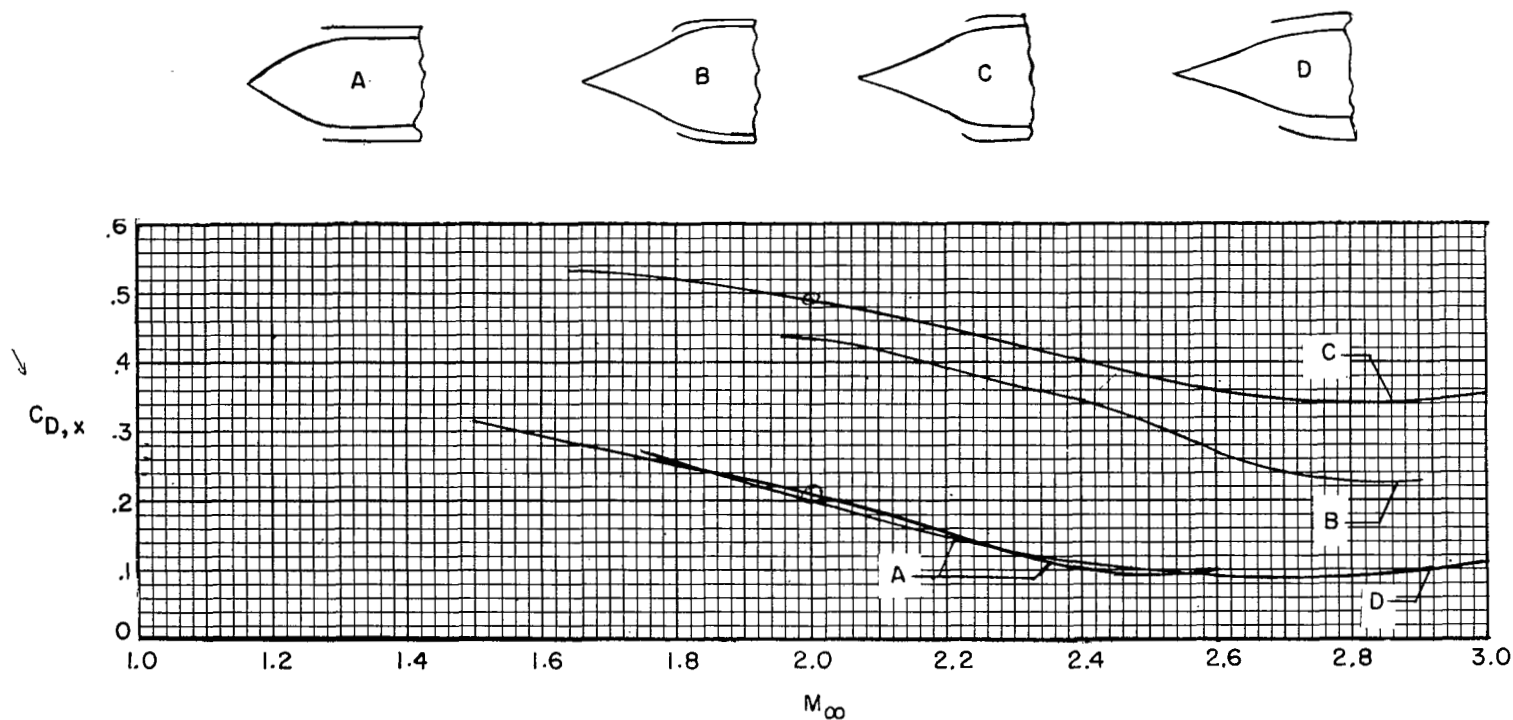


Figure 9.- Summary of inlet external drag as a function of free-stream Mach number for all inlet models.



3 1176 01346 0275

**DO NOT REMOVE SLIP FROM MATERIAL**

Delete your name from this slip when returning material to the library.

NAME	MS
I. Walker	413

NASA Langley (Rev. May 1988)

RIAD N-75

~~CONFIDENTIAL~~